Chinese Chemical Letters 31 (2020) 1535–1539

Contents lists available at ScienceDirect

Chinese Chemical Letters

journal homepage: www.elsevier.com/locate/cclet

Communication

Effective removal of chlorinated organic pollutants by bimetallic iron-nickel sulfide activation of peroxydisulfate

Xuan Yan, Dongting Yue, Chao Guo, Songling Wang, Xufang Qian*, Yixin Zhao*

School of Environmental Science and Engineering, Shanghai Jiao Tong University, Shanghai 200242, China

ARTICLE INFO

Article history:
Received 27 September 2019
Received in revised form 16 October 2019
Accepted 4 November 2019
Available online 5 November 2019

Keywords:
Peroxydisulfate oxidation
Bimetallic iron-nickel sulfide
Chlorinated organic pollutants
Sulfate radicals
Dechlorination

ABSTRACT

Chlorinated organic pollutants (COPs) have caused serious contaminants in soil and groundwater, hence developing methods to remove these pollutants is necessary and urgent. By a simple hydrothermal method, we synthesized the bimetallic iron-nickel sulfide (FeNiS) particles which exhibited excellent catalytic property of COPs removal. FeNiS was chosen as the peroxydisulfate (PDS) activator to removal COPs including 4-chlorophenol (4-CP), 1,4-dichlorophenol (1,4-DCP) and 2,4,6-trichlorophenol (2,4,6-TCP). The results show that FeNiS can efficiently activate PDS to produce sulfate radical ($SO_4^{\bullet-}$) which plays major role in the oxidative dechlorination and degradation due to its strong oxidizing property and the ability of producing hydroxyl radicals ($^{\bullet}OH$) in the alkaline condition. Meanwhile, the Cl^- abscised from COPs during the dechlorination can turn into the chlorine radicals and enhance the degradation and cause further mineralization of intermediate products. This bimetallic FeNiS catalyst is a promising PDS activator for removal of chlorinated organics.

Chlorinated organic pollutants (COPs) as the persistent organic pollutants (POPs) can induce the carcinogenic, teratogenic and mutagenic effects on humans due to their high water solubility and the biological accumulation effect [1–3]. Chlorophenols as the COPs are commonly produced in chemical and pharmaceutical industries like paint, and pesticide, *etc.* [4–6]. The stable C—Cl bond and the position of chlorine atoms relative to the hydroxyl group cause the toxicity and persistence in the biological environment [7].

Sulfate radical ($SO_4^{\bullet-}$) based advanced oxidation processes (AOPs) are proverbially known as promising technologies in organic wastewater treatment [8–10]. $SO_4^{\bullet-}$ exhibits stronger oxidation ability ($E^0 = 2.60–3.10$ eV), more stability over a broad range of pH, and longer half-life ($3–4 \times 10^{-5}$ s) than that of hydroxyl radicals ($^{\bullet}OH$) [11–14]. Transition metal-based materials (Fe, Co and Ni) have been widely used in POPs degradation by catalytically activating radicals [13,15,16]. Many efforts have been made for improving the catalytic activation performances using transition metal-based materials. For example, nano zerovalent iron (nZVI) embedded in porous carbon has showed remarkable performance on peroxydisulfate (PDS) catalytic activation, but it should be protected by organic ligand or porous carbon due to its active reactivity in air [17,18]. Ni is a cheap, earth-abundant element and has lower toxicity compared with Co. And it is widely applied in catalytic reactions. However, neither heterogeneous Ni metal-based catalysts nor the homogeneous Ni^{2+} ion have been discovered to be effective for $SO_4^{\bullet-}$ activation. The low redox potential of Ni/Ni^{2+} in aqueous solution, which is far lower than 1.92 V of Co^{2+}/Co^{3+}, may cause this inactivity for the activation of $SO_4^{\bullet-}$ from peroxymonosulfate (PMS) and PDS [19]. Recently, we found that α-nickel hydroxide and defect-rich NiO can effectively activate PDS to oxidize organic pollutants which was inspired by secondary battery mechanism [20,21]. Bimetallic iron-nickel layered double hydroxide (FeNi LDH) has been applied in the oxygen evolution reaction (OER) electrocatalysts, the introduce of Fe can enhance the electrical conductivity and change the electronic structure [22].

Here, we prepared the FeNiS *via* a modified topotactic conversion reaction using FeNi LDH as a precursor. The sulfidation enhance the electron transfer between Ni and Fe, which can improve the catalytic performance and prolong its service life. Our results show that FeNiS exhibits an enhanced PDS activation performance for the degradation of the pollutants in comparison with FeS and NiS. The pollutant intermediates were detected by gas chromatography mass spectrometry (GCMS). The results indicated the mineralization of COPs. Meanwhile, the Cl^- ions released from chlorophenols can enhance the organic contaminant degradation. Our work demonstrated that bimetallic FeNiS is a promising catalyst for PDS activation and chlorinated organics removal.

* Corresponding authors.
E-mail addresses: qianxufang@sjtu.edu.cn (X. Qian), yixin.zhao@sjtu.edu.cn (Y. Zhao).

https://doi.org/10.1016/j.cclet.2019.11.003

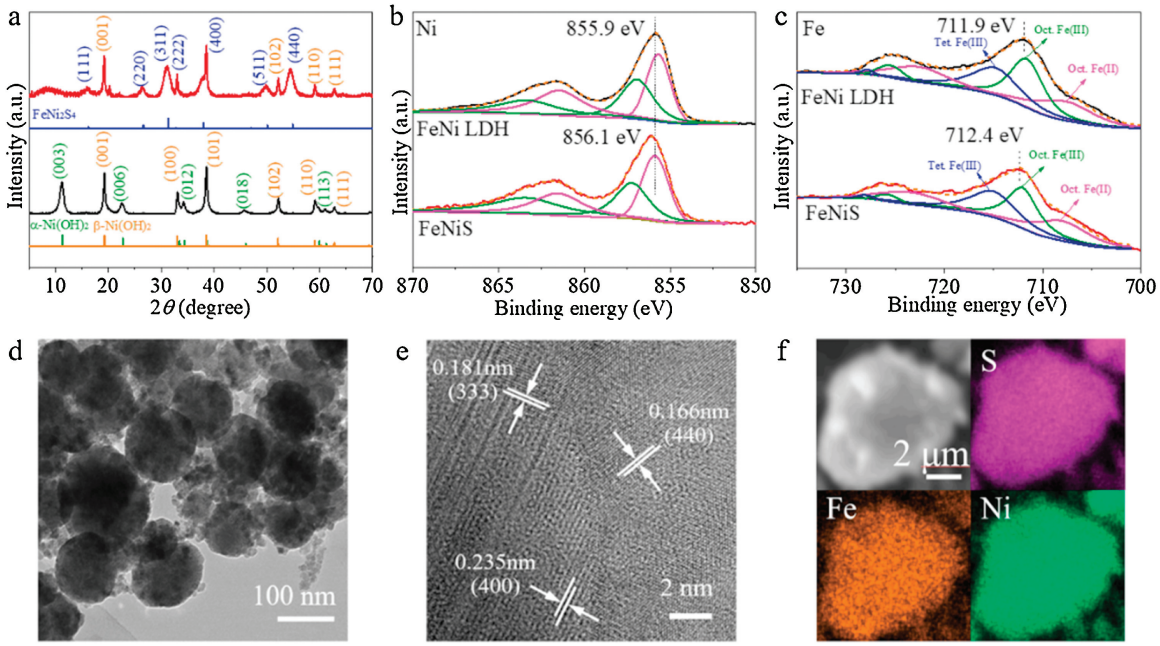

Fig. 1. XRD patterns (a), XPS spectra of Ni (b) and Fe (c) region fitting of FeNi LDH nanosheets and FeNiS nanoparticles, TEM and HRTEM image of FeNiS (d, e), and EDX elemental mapping of FeNiS nanoparticle (f).

The X-ray diffraction (XRD) patterns of FeNi LDH and FeNiS samples are shown in Fig. 1a. The diffraction peaks of the LDH precursor are consisted by (003), (006) and (012) planes of β-$Ni(OH)_2$ and (003), (006), (012), (018) and (113) planes of α-$Ni(OH)_2$ with some planes positively shifted due to the substitution of Fe for Ni. After sulfidation, the FeNiS shows the characteristic diffraction peaks of $FeNi_2S_4$ (JCPDS Card No. 47-1740) with some (001), (102), (110) and (111) planes of β-$Ni(OH)_2$ remained. This indicated that the S can incorporate into FeNi LDH to replace the OH group and then contribute to conversion of FeNi LDH to FeNiS.

The incorporation of S into FeNi LDH is also investigated by the X-ray photoelectron spectroscopy (XPS) (Figs. 1b and c). The Ni 2p XPS can be fitted with one spin-orbit doublet, which is characteristic of Ni(II) (magenta curves) and Ni(III) (green curves) [23]. The deconvoluted Fe $2p_{3/2}$ spectrum displayed the peaks which were assigned to octahedral Fe(II) (magenta curves), octahedral Fe(III) (green curves), and tetrahedral Fe(III) (navy curves), respectively [24–26]. After the sulfidation process for FeNi LDH, both the Ni $2p_{3/2}$ and Fe $2p_{3/2}$ peaks in FeNiS sample are positively shifted, suggesting the change of chemical composition with S incorporation. Both the XRD and XPS results confirm the successful S incorporation in FeNiS samples.

Sphere-like morphology of FeNiS with a diameter about 100 nm is shown in transmission electronic microscopy (TEM) image (Fig. 1d). The high resolution TEM (HRTEM) image (Fig. 1e) shows lattice fringes of 0.166, 0.181 and 0.235 nm which agrees well with that of (440), (511) and (400) planes of FeNiS, respectively. By using the energy dispersive X ray spectroscopy (EDS) measurements, Fe, Ni, and S elements are uniformly distributed throughout the selected area (Fig. 1f). The Fe/Ni atomic ratio was about 3/10, which

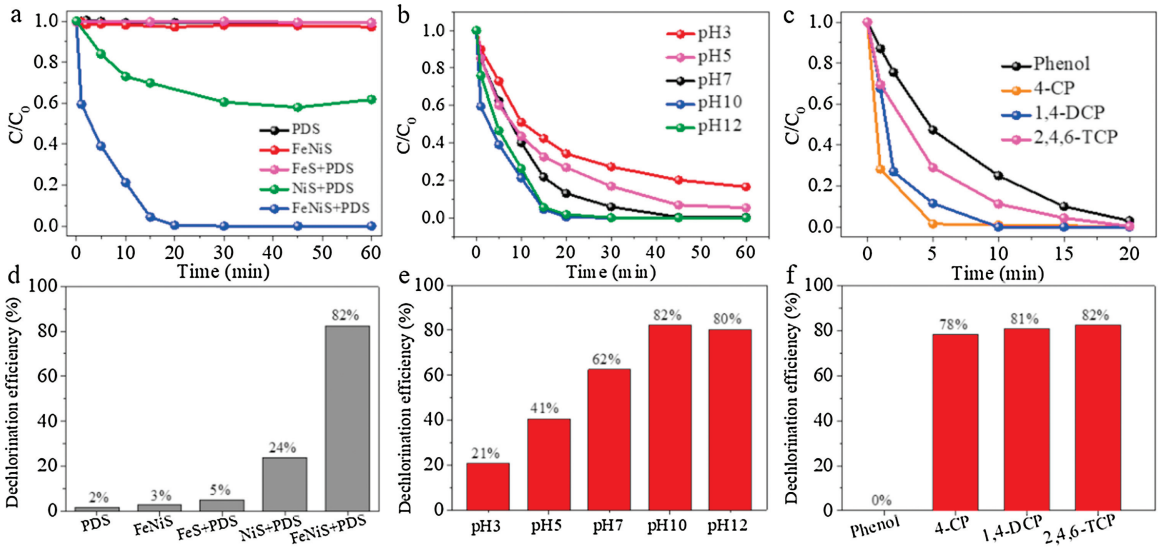

Fig. 2. The removal and dechlorination efficiency of TCP in different reaction systems (a, d), and at different pH in FeNiS/PDS system (b, e). The removal and dechlorination efficiency of phenol, 1-CP, 1,4-DCP, 2,4,6-TCP (c, f). Reaction conditions: pH 10, PDS dosage 0.5 g/L, catalyst dosage 0.25 g/L, and pollutants dosage 50 mg/L.

is consistent with the XPS result (Table S1 in Supporting information).

The trichlorophenol (TCP) oxidation performance of FeNiS and the control blank experiments of PDS activation were implemented. Neither PDS nor FeNiS alone was active for TCP oxidation (Fig. 2a). Monometallic sulfide FeS shows negative performance in activating PDS and only 38% of TCP was degraded in NiS/PDS system. The degradation efficiency of TCP was greatly improved in bimetallic FeNiS/PDS system, which was degraded completely within 20 min. Fig. S1 (Supporting information) shows that the optimal PDS dosage is 0.3 g/L. The FeNiS/PDS system also exhibits the best efficiency for TCP dechlorination (82%) (Fig. 2d).

pH Values of the pollutant solution are always important for PDS activation [27]. In the present research, we measured the TCP oxidation performance by catalytic PDS activation at different pH values. The TCP removal efficiency decreases with the decrease of pH value (Fig. 2b). But even in the acid condition, 81% of TCP was removed in 60 min. FeNiS exhibits the highest TCP removal efficiency (82%) at pH 10 and then greatly decreased (21%) at pH 3 (Fig. 2e). The results indicate that the activation of PDS by bimetallic sulfide FeNiS induces more efficient TCP oxidation in alkaline condition.

To better evaluate the catalytic performance of FeNiS/PDS system, we further test the degradation of some other organic pollutants such as phenol, 4-chlorophenol (4-CP), and 1,4-dichlorophenol (1,4-DCP). This system shows excellent degradation ability for these organic pollutants, which were fully degraded within 20 min (Fig. 2c). FeNiS shows high dechlorination efficiency for 4-CP, 1,4-DCP, and 2,4,6-TCP (78%, 81%, and 82% respectively) under the optimal degradation condition (Fig. 2f).

The radicals generated during the PDS activation were detected by electron paramagnetic resonance (EPR). Fig. 3a shows the DMPO-SO_4 (1:1:1:1:1:1) and DMPO-OH (1:2:2:1) signals, which verified that FeNiS can activate PDS to produce $SO_4^{\bullet-}$ and $^{\bullet}OH$. The chloric organic compounds adsorbed onto the surface of the FeNiS nanoparticles were efficiently oxidized, thus the Cl^- was removed by the oxidative dechlorination in the presence of $SO_4^{\bullet-}$ and $^{\bullet}OH$ radicals (Figs. 3a and d) [11,28,29]. The intermediate products in TCP degradation was investigated by GCMS analysis. As shown in Fig. S2 (Supporting information), trans-1,2-dichloro-cyclopentane, *trans*-chlorocyclopentane, toluene, and chloro-benzene, were detected after 15 min, which confirmed the effectively oxidative dechlorination performance of FeNiS/PDS. Some small molecular acids like propanoic acid-ethyl ester and isopropyl acetate were also produced. More than 80% of the total organic carbon (TOC) was removed within 60 min, which was more robust than that of the most sulfide bimetallic-based heterogeneous catalysts (Table S2 in Supporting information). We also tried to track the presence of $^{\bullet}Cl$ which can be generated from the released anions Cl^- by free radical quenching experiment using ethanol. Ethanol possesses a high reactivity with $SO_4^{\bullet-}$ ($k = 1.6 \times 10$ L mol^{-1} s^{-1}) and an obviously inhibitory effect was observed when the pollutant is phenol [30]. However, ethanol exhibits negligible impact on TCP degradation (Fig. 3b). One reason according to conjecture is that the $SO_4^{\bullet-}$ was preferentially react with Cl^- ($k = 4.7 \times 10^8$ L mol^{-1} s^{-1}) to produce $^{\bullet}Cl$ at low Cl^- concentrations rather than extinguished by ethanol ($k = 1.6 \times 10^7$ L mol^{-1} s^{-1}) [31]. For better investigating the role of Cl^-, we have investigated the effect of different Cl^- concentration on phenol degradation efficiency in the presence of ethanol. The phenol degradation efficiency in FeNiS/PDS system can be enhanced with the addition of low Cl^- concentrations (0.25 mmol/L and 0.5 mmol/L), but a higher Cl^- concentration (above 1.0 mmol/L Cl^-) has lower positive effects on phenol degradation (Fig. 3c). This result confirmed that Cl^- can be translated into .Cl and then transferred to $^{\bullet}OH$ and $S_2O_8^{\bullet-}$ (Eqs. 1–3), which can inhibit the oxidative radical quenching by ethanol. This process provides another route for oxidative radical, thereby enhancing the chloric organic compounds degradation even in the presence of scavengers. A high concentration of Cl^- favors the generation of $Cl_2^{\bullet-}$ ($E_0 = 2.3$ V), which has a much lower reaction rate constant with PDS ($k < 1 \times 10^4$ L mol^{-1} s^{-1}; Eqs. 4 and 5) [32,33]. We also evaluated the oxidation performance of FeNiS/PDS for different COPs. Figs. 2c and f show that 4-CP, 1,4-DCP, and 2,4,6-TCP were more efficiently removed by FeNiS/PDS system than the case of phenol. The above results indicate that the Cl^- released from chloric organic compounds can be translated into $^{\bullet}Cl$, which maybe further transfer to $^{\bullet}OH$ and $S_2O_8^{\bullet-}$ for enhancing the chloric organic compounds degradation (Eqs. 3–5) [31,33–36].

The proposed mechanism of FeNiS/PDS catalytic oxidation process was shown in Fig. 3d. In FeNiS/PDS system, Ni(II) activates $S_2O_8^{2-}$ to produce $SO_4^{\bullet-}$ and Ni(II) was oxidized into Ni(III). Ni(III)/Ni(II) redox in FeNiS/PDS system was induced by the chemical reactions with PDS (Eqs. 6–8) [32,37–39]. The formation of $^{\bullet}OH$ was attributed to the conversion of $SO_4^{\bullet-}$ into $^{\bullet}OH$ under alkaline conditions (Eqs. 9, 10) [31,32]. Therefore, FeNiS/PDS system in alkaline condition exhibits better catalytic performance for TCP degradation than that in the acid condition (Figs. 2b and e).

$$SO_4^{\bullet-} + Cl^- \rightarrow Cl^{\bullet} + SO_4^{2-},\ k_{SO_4^{\bullet-}+Cl^-} = 3 \times 10^8\ \text{L mol}^{-1}\ \text{s}^{-1} \quad (1)$$

$$Cl^{\bullet} + S_2O_8^{2-} \rightarrow S_2O_8^{\bullet-} + Cl^- \quad (2)$$

$$Cl^{\bullet} + OH^- \rightarrow ClHO^{\bullet},\ k_{Cl^{\bullet}+OH^-} = 1.8 \times 10^{10}\ \text{L mol}^{-1}\ \text{s}^{-1} \quad (3)$$

$$Cl^{\bullet} + Cl^- \rightarrow Cl_2^{\bullet-},\ k_{Cl^{\bullet}+Cl^-} = 8 \times 10^9\ \text{L mol}^{-1}\ \text{s}^{-1} \quad (4)$$

$$Cl_2^{\bullet-} + S_2O_8^{2-} \rightarrow S_2O_8^{\bullet-} + 2Cl^- \quad (5)$$

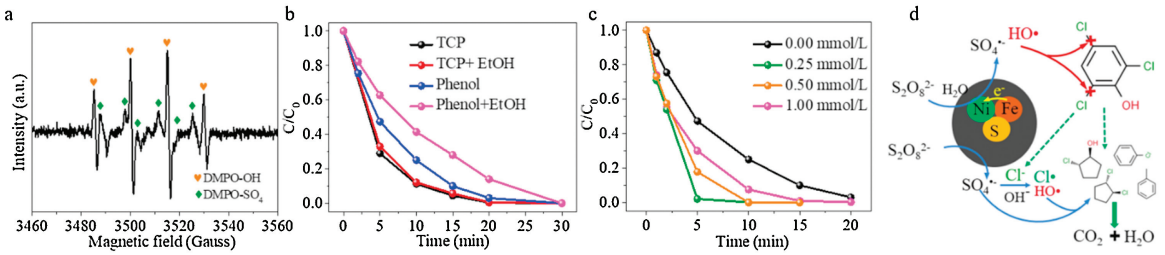

Fig. 3. DMPO spin-trapping EPR spectra (a), the TCP and phenol removal efficiency with and without EtOH (b), and the phenol removal efficiency with different dosage of NaCl in the presence of ethanol (c). Proposed mechanism of the dechlorination and degradation of TCP (d).

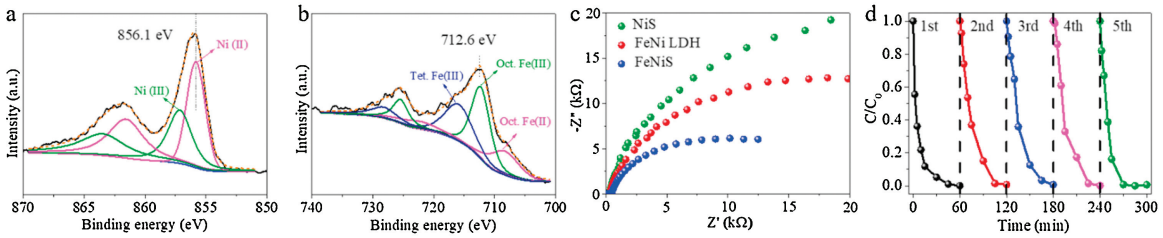

Fig. 4. XPS spectra of Ni (a) and Fe (b) region fitting of FeNiS nanoparticles after 5 times cycle use; EIS spectra of FeNiS, FeNi LDH, and NiS (c); repeated degradation of TCP by FeNiS/PDS system (d). Reaction conditions: pH 10, PDS dosage 0.5 g/L, catalyst dosage 0.25 g/L, TCP dosage 50 ppm.

$$Ni(II) + S_2O_8^{2-} \rightarrow Ni(III) + SO_4^{\bullet-} + SO_4^{2-} \quad (6)$$

$$Ni(III) + S_2O_8^{2-} \rightarrow Ni(II) + S_2O_8^{\bullet-} \quad (7)$$

$$Ni(III) + S_2O_8^{\bullet-} + 2H_2O \rightarrow Ni(II) + 2HSO_5^- + 2H^+ \quad (8)$$

$$SO_4^{\bullet-} + H_2O \rightarrow SO_4^{2-} + HO^{\bullet} + H^+, \quad k_{SO_4^{\bullet-} + H_2O} < 1.0 \times 10^3 \ L \ mol^{-1} \ s^{-1} \quad (9)$$

$$SO_4^{\bullet-} + OH^- \rightarrow HO^{\bullet} + SO_4^{2-}, \quad k_{SO_4^{\bullet-} + OH^-} = 6.5 \times 10^7 \ L \ mol^{-1} \ s^{-1} \quad (10)$$

The enhanced PDS activation after sulfidation treatment was also explored. XPS results indicated that 7% of the total Fe was transformed from octahedral Fe(III) to octahedral Fe(II) after the sulfidation process (Table S3 in Supporting information), which can improve the reduction of Ni(III) (Eq. 11) [27]. After the catalytic reaction, the 4% of Fe(II) was transferred into Fe(III), while the atom ratio of Ni(II) to Ni(III) remained constant (Figs. 4a and b and Table S3). These results demonstrated that Fe in FeNiS can prevent the accumulation of high-valent Ni(III) centers, thereby enhancing the Ni(III)/Ni(II) cycle for PDS activation.

$$Fe(II) + Ni(III) \rightarrow Fe(III) + Ni(II) \quad (11)$$

The electrochemical impendence spectra (EIS) spectrum in Fig. 4c shows that FeNiS catalyst features the smallest R_{ct} at catalyst/electrolyte interface than that of other two catalysts (NiS and FeNi LDH), indicating the Fe introduction and sulfidation treatment can result in a more facile charge transfer kinetics. Catalyst stability was also evaluated (Fig. 4d and Fig. S3 in Suppoprting information), the results show that FeNiS remains the same catalytic performance even after five cycles and so was the dechlorination stability. The reaction kinetics was also calculated to visualize the recyclability (Fig. S4 in Supporting information). All these results indicated that FeNiS with prominent ability of sulfate radical activation would be a hopeful catalyst for chloric organic compounds pollution purification.

In summary, the bimetallic FeNiS particles were successfully prepared via a facile hydrothermal method. The formed FeNiS nanoparticles provide an efficient electron transfer between nickel and iron, which contributed to the high catalytic dechlorination property for chloric organic compounds. The FeNiS/PDS system presents a high mineralization activity for organic pollutants and the Cl^- released from chloric organic compounds can further enhance the organic contaminant degradation. This work confirmed that the FeNiS nanoparticles with catalytic oxidative dechlorination property, PDS activation performance, and durability, are a promising catalyst for chloric organic compounds degradation. It is believed that the concept of rational design and effective synthesis of bimetallic nanoparticles can be a promising strategy for environmental remediation.

Declaration of competing interest

The contents of this manuscript have not been copyrighted or published previously. The authors declare no competing financial interest.

Acknowledgments

This work was supported by the National Natural Science Foundation of China (Nos. 21806106, 51861145101, 21777096 and 21777097), Shanghai Shuguang Grant (No. 17SG11) and the China Postdoctoral Science Foundation (Nos. 2017M621483 and 2018T110397).

Appendix A. Supplementary data

Supplementary data associated with this article can be found, in the online version, at https://doi.org/10.1016/j.cclet.2019.11.003.

References

[1] A. Sorokin, S. De Suzzoni-Dezard, D. Poullain, et al., J. Am. Chem. Soc. 118 (1996) 7410–7411.
[2] U.I. Gaya, A.H. Abdullah, M.Z. Hussein, Z. Zainal, Desalination 263 (2010) 176–182.
[3] B.H. Hameed, I.A.W. Tan, A.L. Ahmad, Chem. Eng. J. 144 (2008) 235–244.
[4] M. Vinita, R.P.J. Dorathi, K. Palanivelu, Sol. Energy 84 (2010) 1613–1618.
[5] C.G. Joseph, G.L. Puma, A. Bono, et al., Desalination 276 (2011) 303–309.
[6] G. Díaz-Díaz, M. Celis-García, M.C. Blanco-López, et al., Appl. Catal. B: Environ. 96 (2010) 51–56.
[7] Y.M. Tzou, S.L. Wang, J.C. Liu, et al., J. Hazard. Mater. 152 (2008) 812–819.
[8] C. Fang, D. Xiao, W. Liu, et al., Chemosphere 144 (2016) 2415–2420.
[9] J. Deng, M. Xu, C. Qiu, et al., Appl. Surface Sci. 459 (2018) 138–147.
[10] H. Zhang, Q. Ji, L. Lai, et al., Chin. Chem. Lett. 30 (2019) 1129–1132.
[11] K. Govindan, M. Raja, M. Noel, E.J. James, J. Hazard. Mater. 272 (2014) 42–51.
[12] J.E. Silveira, T.O. Cardoso, M. Barretorodrigues, et al., Environ. Technol. 39 (2017) 1208–1216.
[13] C. Luo, J. Gao, D. Wu, et al., Chem. Eng. J. 358 (2019) 1342–1350.
[14] F. Ghanbari, M. Moradi, F. Gohari, J. Water. Process. Eng. 9 (2016) 22–28.
[15] M. Pera-Titus, V. Garcı'a-Molina, M.A. Baños, et al., Appl. Catal. B: Environ. 47 (2004) 219–256.
[16] Q. Gong, Y. Liu, Z. Dang, J. Hazard. Mater. 371 (2019) 677–686.
[17] Y. Wu, X. Chen, Y. Han, et al., Environ. Sci. Technol. 53 (2019) 9081–9090.
[18] C. Kim, J.Y. Ahn, T.Y. Kim, et al., Environ. Sci. Technol. 52 (2018) 3625–3633.
[19] T. Simon, N. Bouchonville, M.J. Berr, et al., Nat. Mater. 13 (2014) 1013–1018.
[20] D. Yue, X. Qian, M. Ren, et al., Sci. Bull. 63 (2018) 278–281.
[21] X. Long, G. Li, Z. Wang, et al., J. Am. Chem. Soc. 137 (2015) 11900–11903.
[22] L. Trotochaud, S.L. Young, J.K. Ranney, S.W. Boettcher, J. Am. Chem. Soc. 136 (2014) 6744–6753.
[23] C. Yuan, J. Li, L. Hou, et al., Adv. Funct. Mater. 22 (2012) 4592–4597.
[24] D. Wilson, M.A. Langell, Appl. Surface Sci. 303 (2014) 6–13.
[25] A. Petran, T. Radu, B. Culic, R. Turcu, Appl. Surface Sci. 390 (2016) 1–6.

[26] J.E. Thomas, W.M. Skinner, R.St.C. Smart, Geochim. Cosmochim. Acta 67 (2003) 831–843.
[27] G.X. Huang, C.Y. Wang, C.W. Yang, et al., Environ. Sci. Technol. 51 (2017) 12611–12618.
[28] C.X. Li, Y.J. Wang, C.B. Chen, et al., Sci. Total Environ. 664 (2019) 133–139.
[29] L. Xu, R. Yuan, Y. Guo, et al., Chem. Eng. J. 217 (2013) 169–173.
[30] W.D. Oh, Z. Dong, T.T. Lim, Appl. Catal. B: Environ. 194 (2016) 169–201.
[31] W.J. McElroy, J. Phys. Chem. 94 (1990) 2435–2441.
[32] C. Zhu, F. Zhu, C. Liu, et al., Environ. Sci. Technol. 52 (2018) 8548–8557.
[33] X.Y. Yu, Z.C. Bao, J.R. Barker, J. Phys. Chem. A 108 (2004) 295–308.
[34] U.K. Kläning, T. Wolf, Ber. Bunsenges. Phys. Chem. 89 (1985) 243–245.
[35] R. Mertens, C. von Sonntag, J. Photochem. Photobiol. A 85 (1995) 1–9.
[36] D. Wang, J.R. Bolton, R. Hofmann, Water Res. 46 (2012) 4677–4686.
[37] A. Tsitonaki, B. Petri, M. Crimi, et al., Crit. Rev. Environ. Sci. Technol. 40 (2010) 55–91.
[38] H. Liu, T.A. Bruton, F.M. Doyle, D.L. Sedlak, Environ. Sci. Technol. 48 (2014) 10330–10336.
[39] V. Lepentsiotis, J. Domagala, I. Grgic, et al., Inorg. Chem. 38 (1999) 3500–3505.